nature biotechnology

ANALYSIS

Deconvolution of complex G protein–coupled receptor signaling in live cells using dynamic mass redistribution measurements

Ralf Schröder[1,5], Nicole Janssen[2,5], Johannes Schmidt[1], Anna Kebig[2], Nicole Merten[1], Stephanie Hennen[1], Anke Müller[1], Stefanie Blättermann[1], Marion Mohr-Andrä[2], Sabine Zahn[3], Jörg Wenzel[3], Nicola J Smith[4], Jesús Gomeza[1], Christel Drewke[1], Graeme Milligan[4], Klaus Mohr[2] & Evi Kostenis[1]

Label-free biosensor technology based on dynamic mass redistribution (DMR) of cellular constituents promises to translate GPCR signaling into complex optical 'fingerprints' in real time in living cells. Here we present a strategy to map cellular mechanisms that define label-free responses, and we compare DMR technology with traditional second-messenger assays that are currently the state of the art in GPCR drug discovery. The holistic nature of DMR measurements enabled us to (i) probe GPCR functionality along all four G-protein signaling pathways, something presently beyond reach of most other assay platforms; (ii) dissect complex GPCR signaling patterns even in primary human cells with unprecedented accuracy; (iii) define heterotrimeric G proteins as triggers for the complex optical fingerprints; and (iv) disclose previously undetected features of GPCR behavior. Our results suggest that DMR technology will have a substantial impact on systems biology and systems pharmacology as well as for the discovery of drugs with novel mechanisms.

G protein–coupled receptors (GPCRs) are among the most important drug target classes[1]. For many members of this receptor family, it is now well established that they oscillate among multiple conformations that can be differentially stabilized by ligands, thus permitting access to only a subset of the complete repertoire of receptor behaviors[2–8]. This phenomenon, also referred to as biased agonism or functional selectivity, has important implications for GPCR-related drug discovery because it raises the possibility to design signaling pathway–specific therapeutics.

Activation of downstream signaling events of GPCRs has been traditionally recorded with assays based on quantification of distinct intracellular second messengers[5,9–11] and/or translocation of β-arrestin proteins[5,12–16]. It is becoming increasingly apparent, however, that integrated cellular responses—rather than individual components of signaling pathways—need to be analyzed, because different classes of GPCRs typically produce one or more specific second messengers and because GPCRs may engage additional non–G protein effectors[17–21]. An optical biosensor technology, based on measurement of the cellular process of dynamic mass redistribution, was recently developed to monitor such integrated signaling responses. In DMR technology, polarized light is passed through the bottom of a biosensor microtiter plate containing the cell samples, and a shift in wavelength of reflected light is indicative of redistribution of cellular constituents triggered upon receptor activation (**Fig. 1a**)[5,22,23]. The wavelength shift may vary in magnitude, direction (positive or negative) and over time depending on how different activated signaling pathways cause various intracellular molecules to relocate.

DMR technology enables GPCR function to be analyzed without labeling. In the assay, receptor activity is measured as an optical trace that represents the generic response of living cells, reminiscent of the holistic responses obtained in tissue or organ bath experiments. Label-free technologies could therefore be decisively advantageous to monitor even complex signaling processes, particularly in primary cells, which are difficult to analyze with traditional biochemical methods and which are difficult to transfect with labeled components of the GPCR signaling cascade for optical studies[23–25]. It is likely that these obstacles have so far precluded assessment of drug candidates in their native environment.

Although label-free recording of DMR is already being applied in pharmaceutical companies on a more empirical basis to assess feasibility for high-throughput screening or for pharmacological ligand profiling[25–29], no in-depth analytical study had been conducted that compared this technology platform with the methods traditionally used in early drug discovery.

Therefore, we applied DMR to monitor signaling of a number of GPCRs from all four coupling classes (G_i/G_o, G_s, G_q and G_{12}/G_{13}) and compared the receptor's functionality for inducing a whole-cell response with the more classical biochemical approaches to define GPCR signal transduction. An experimental strategy is presented to identify the post-receptor trigger underlying the optical response profiles, thereby allowing optical traces to be precisely assigned to distinct GPCR-mediated signaling pathways. We then take advantage

[1]Molecular, Cellular, and Pharmacobiology Section, Institute of Pharmaceutical Biology, University of Bonn, Bonn, Germany. [2]Pharmacology and Toxicology Section, Institute of Pharmacy, University of Bonn, Bonn, Germany. [3]Department of Dermatology, University of Bonn, Bonn, Germany. [4]Molecular Pharmacology Group, Neuroscience and Molecular Pharmacology, Faculty of Biomedical and Life Sciences, University of Glasgow, Glasgow, UK. [5]These authors contributed equally to this work. Correspondence should be addressed to E.K. (kostenis@uni-bonn.de) or K.M. (k.mohr@uni-bonn.de).

Published online 15 August 2010; doi:10.1038/nbt.1671

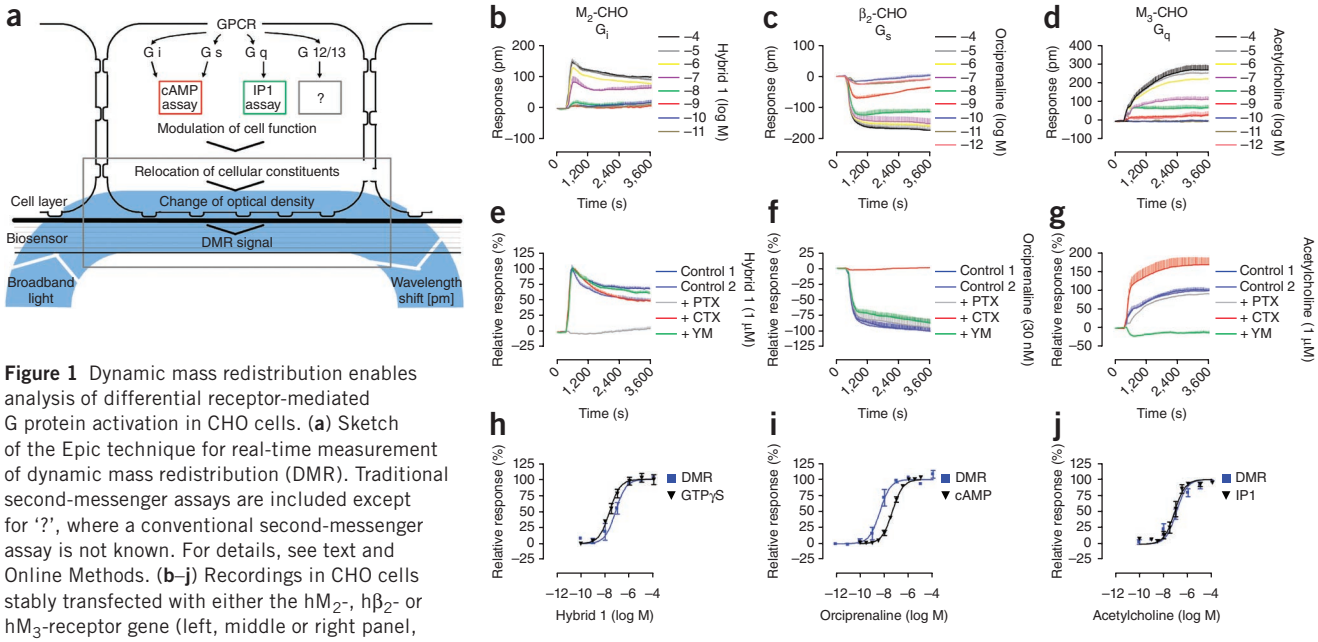

Figure 1 Dynamic mass redistribution enables analysis of differential receptor-mediated G protein activation in CHO cells. (**a**) Sketch of the Epic technique for real-time measurement of dynamic mass redistribution (DMR). Traditional second-messenger assays are included except for '?', where a conventional second-messenger assay is not known. For details, see text and Online Methods. (**b**–**j**) Recordings in CHO cells stably transfected with either the hM_2-, $h\beta_2$- or hM_3-receptor gene (left, middle or right panel, respectively). (**b**–**d**) The cell lines were challenged with the indicated concentrations of the corresponding agonist (M_2, hybrid 1; β_2, orciprenaline; M_3, acetylcholine), and wavelength shift was monitored as a measure of receptor activation. Representative data (mean + s.e.m.) of at least four independent experiments. (**e**–**g**) Validation by toxin pretreatment of agonist-induced G_i, G_s and G_q activation: pertussis toxin (100 ng/ml; PTX), cholera toxin (100 ng/ml; CTX), YM 254890 (300 nM; YM). Representative data (mean + s.e.m.) from at least three independent experiments. Control 1 corresponds to YM signature and control 2 to PTX and CTX signatures. (**h**–**j**) Comparison of concentration-effect curves resulting from DMR assays and traditional assays. Calculated log EC_{50} values are: (**h**) M_2 DMR: −7.21 ± 0.27, GTPγS: −7.63 ± 0.07; (**i**) β_2 DMR: −8.35 ± 0.24, cAMP: −7.34 ± 0.03; (**j**) M_3 DMR: −7.02 ± 0.08, IP1: −7.02 ± 0.07. All data are means (±s.e.m.) of at least three independent experiments.

of this strategy to explore complex GPCR signaling patterns in both recombinant and primary human cells. Notably, our results provide evidence that simultaneous visualization of signaling pathways by DMR, but not by recording of defined downstream signaling events in single component functional assays, enables unexpected signaling phenomena to be identified, thus implying the need to shift from single-component to system analysis. We suggest that optical recording of DMR represents an enabling technology with substantial impact on both the dissection of complex biological signaling patterns of GPCRs in basic research and the understanding of mechanisms of drug action in GPCR drug discovery.

RESULTS

DMR reports signaling of G_i/G_o-, G_s- and G_q-linked receptors

To establish that DMR measures signaling downstream of different G protein classes, CHO cells stably transfected to express the G_i/G_o-sensitive muscarinic receptor M_2, the G_q-linked muscarinic receptor M_3, or the G_s-sensitive adrenergic β_2 receptor were challenged with increasing concentrations of their respective agonists, and DMR was recorded as a function of receptor activity. For all three receptors, real-time optical recordings were concentration dependent and varied depending on the primary signaling pathway of each receptor (**Fig. 1b–d**). Ligand activity was undetectable in native CHO cells, demonstrating that the DMR traces required the presence of the respective GPCRs (**Supplementary Fig. 1**).

To further establish whether heterotrimeric G proteins are responsible for orchestrating the observed temporal response patterns, we chose to pharmacologically silence the G protein signaling pathways using pertussis toxin (PTX) to block G_i/G_o signaling, YM-254890 (hereafter referred to as YM) to suppress G_q signaling (ref. 30), and cholera toxin (CTX) to mask G_s signaling. Indeed, M_2 receptor traces were completely abrogated by PTX but unaffected by YM and CTX (**Fig. 1e**), identifying G_i/G_o proteins as upstream triggers for this optical fingerprint. On their own, PTX, YM or CTX did not induce a DMR response (**Supplementary Fig. 2**). Furthermore, G protein activation, as reflected by GTPγS binding assays, was in good agreement with the DMR data (**Fig. 1**), thus supporting the notion that the optical traces resulted from a G_i-mediated signaling event. Corresponding observations were made for G_s- and G_q-DMR assays: the G_s signatures of the β_2 receptor were exclusively masked by CTX but not by PTX or YM (**Fig. 1f**), and the G_q signatures of the M_3 receptor were masked by YM but not by PTX or CTX (**Fig. 1g** and **Supplementary Fig. 3**). Again, traditional second-messenger assays suggested that optical traces are a consequence of engaging the respective signaling pathways assigned to both receptors (**Fig. 1i,j**).

DMR can identify signaling along the G_{12}/G_{13} pathway

Whereas second-messenger assays are well suited to detect activation of G_i-, G_s- and G_q-sensitive receptors, such assays are not yet available to detect G_{12}/G_{13} signaling, apart from high-content screening or approaches that assume contribution of these G proteins by recording mostly far removed downstream events[31]. To demonstrate that DMR provides information about signaling through this fourth Gα protein family, we took advantage of the atypical cannabinoid receptor GPR55, which is the only GPCR known to date with exclusive bias toward the G_{12}/G_{13} pathway[8,32,33]. Human embryonic kidney (HEK293) cells were chosen to establish a stable GPR55-expressing clone, because these cells were virtually unresponsive in DMR assays to lysophosphatidylinositol (LPI), currently the most suitable GPR55 agonist[32–34] (**Supplementary Fig. 4a**). Of note, wild-type CHO cells responded with robust

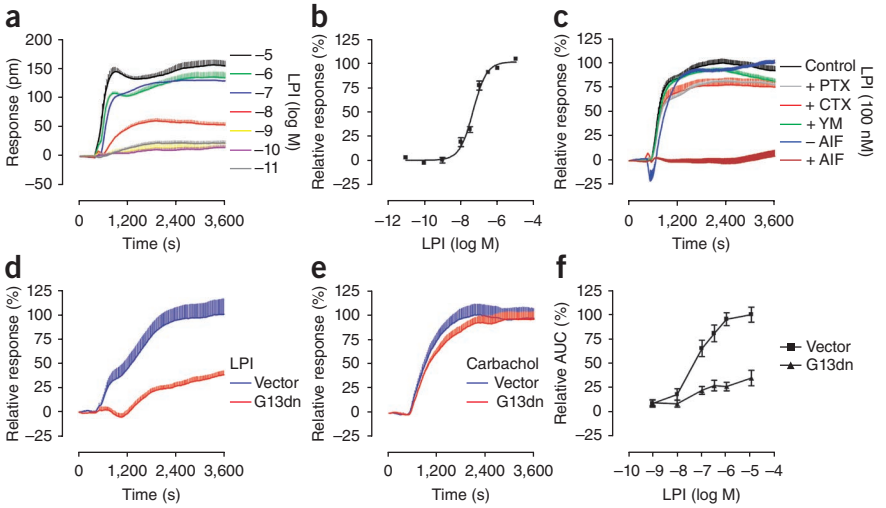

Figure 2 Dynamic mass redistribution visualizes signaling along the G_{12}/G_{13} pathway. (**a**) GPR55-HEK cells were challenged with the indicated concentrations of the GPR55 agonist lysophosphatidylinositol (LPI), and wavelength shift was monitored over time as a measure of receptor activation. Data shown are representative (mean + s.e.m.) of at least three independent experiments. (**b**) Concentration-effect curve for LPI in GPR55-HEK cells resulting from DMR traces in three independent experiments. The calculated log EC_{50} value is -7.34 ± 0.05. (**c**) LPI-mediated alteration of cell activity in GPR55-HEK cells is not blunted by pretreatment with toxin (5 ng/ml PTX, 100 ng/ml CTX) or pathway inhibitor (300 nM YM-254890), but is sensitive to preincubation of cells with 300 μM of the pan–G protein agonist AlF_4^- (AlF). Shown are representative data (mean + s.e.m.) from at least three independent experiments. (**d**–**f**) LPI- but not carbachol-mediated DMR is substantially diminished in GPR55-HEK cells cotransfected to express a dominant negative form of G13 (G13dn, G13Q226L,D294N). GPR55 cells cotransfected to express G13dn or empty pcDNA3.1 vector DNA were treated with 1 μM LPI (**d**) or 100 μM carbachol (**e**) and DMR was monitored over time. Depicted are representative optical traces (**d**,**e**) and concentration effect relationships of five such experiments (**f**).

DMR signals to LPI challenge, whereas the same cells did not show any significant LPI effect in traditional second-messenger assays covering the G_i, G_s and G_q pathways and were therefore judged unsuitable for transfection with and functional exploration of GPR55 (**Supplementary Fig. 4b–d**). GPR55-HEK cells displayed concentration-dependent optical traces upon exposure to LPI (**Fig. 2a**,**b**). Notably, GPR55-mediated DMR was insensitive to inhibition of G_i, G_s or G_q signaling by PTX, CTX or YM, but was silenced when cells were pretreated with the pan–G protein activator aluminum fluoride (AlF_4^-) (**Fig. 2c**). This effect could not be explained by a general blunting of cell responsiveness in DMR assays (**Supplementary Fig. 5**). These data suggest a G-protein origin of the GPR55 trace that is independent of coupling to G_i/G_o, G_s and G_q proteins, a conclusion that is further corroborated by the lack of second-messenger production in GPR55-HEK cells (**Supplementary Fig. 6**). Notably, GPR55-HEK cells transfected to coexpress dominant negative G13 (G13dn, G13Q226L,D294N) did not display altered GPR55 cell surface expression (**Supplementary Fig. 7**) but did show substantially diminished LPI-induced DMR responses, whereas optical traces elicited by carbachol to stimulate endogenously expressed G_q-sensitive muscarinic receptors, as a control, were virtually unaffected (**Fig. 2d–f**). Taken together, these data suggest that DMR is competent to visualize signaling along the G_{12}/G_{13} pathway and therefore represents a methodology applicable to probe functionality of GPCRs from all four coupling classes, which at present is beyond reach of most GPCR assay platforms.

DMR response profiles are cell type dependent

As signaling-dependent relocation of cellular constituents is likely to depend on cellular background, we also examined G_i/G_o-, G_q- and G_s-mediated DMR responses in HEK293 cells. The G_i-coupled prostaglandin D_2 receptor CRTH2 revealed a signature profile comparable to that observed for the G_i-coupled M_2 receptor in CHO cells (**Fig. 3a**; compare **Fig. 1b**). Similar DMR traces were also obtained when a panel of additional G_i/G_o-coupled receptors were analyzed (**Supplementary Fig. 8**), supporting the notion that optical traces may indeed be suggestive of engagement of particular signaling pathways. However, a positive DMR signal was observed when the G_s signaling cascade was activated in HEK cells by the lipid mediator prostaglandin E_1 (PGE_1), which acts via the two endogenously expressed G_s-linked EP2-EP4 receptors, or by orciprenaline, which stimulates endogenous β_2 receptors (**Fig. 3** and **Supplementary Fig. 9**); this was in contrast to the downward-deflected G_s signature in CHO cells (**Fig. 1c**). Similar cellular context dependency was also observed when forskolin, a direct adenylyl cyclase activator that bypasses the receptor, was applied. DMR responses of forskolin are essentially superimposable on those induced by stimulation of G_s GPCR agonists in both CHO and HEK293 cells (**Supplementary Fig. 10**). Differentiation of signatures with pathway modulators (**Fig. 3b–d**,**g–i**), specific receptor antagonists (data not shown) and second-messenger assays (**Fig. 3e**,**j**) confirmed and validated that optical traces for the tested receptors faithfully reflect stimulation of signaling pathways previously assigned to them. Taken together, these disparate DMR measurements suggest that unique differences exist in the spatiotemporal organization of the G_s downstream signaling network in these two cell lines.

Holistic DMR recordings uncover signaling promiscuity

The free fatty acid receptor FFA1 has previously been classified as a G_q/G_{11} sensitive receptor[35–37]. Stimulating FFA1-HEK cells with the small-molecule agonist TUG424 (ref. 38) induced robust DMR responses, distinct in shape from those obtained for G_i- and G_s-coupled receptors in this cellular background (compare **Fig. 4a** with **Fig. 3a**,**f**). However, unlike what would be expected for a G_q-sensitive receptor, FFA1-mediated DMR was only partly sensitive to inhibition by the G_q inhibitor YM (**Fig. 4b**; compare black and blue trace), although the same concentration of YM was sufficient to completely silence FFA1 activity in assays quantifying generation of inositol phosphates (IP1 assays), the classical approach to measure functional activity of G_q/G_{11}-sensitive receptors (**Fig. 4c**). Apparently, FFA1 engages signaling pathways in addition to the G_q/G_{11} pathway in this particular cellular background. Indeed, FFA1 also signals through the G_i pathway, as inferred from both the partial PTX sensitivity of the DMR signal (**Fig. 4b**; compare black and gray trace) and the partial inhibition by PTX of ERK1/2 MAP kinase phosphorylation (**Supplementary Fig. 11**). In agreement with a dual G_q/G_i coupling profile, only the combination of PTX and YM was required and

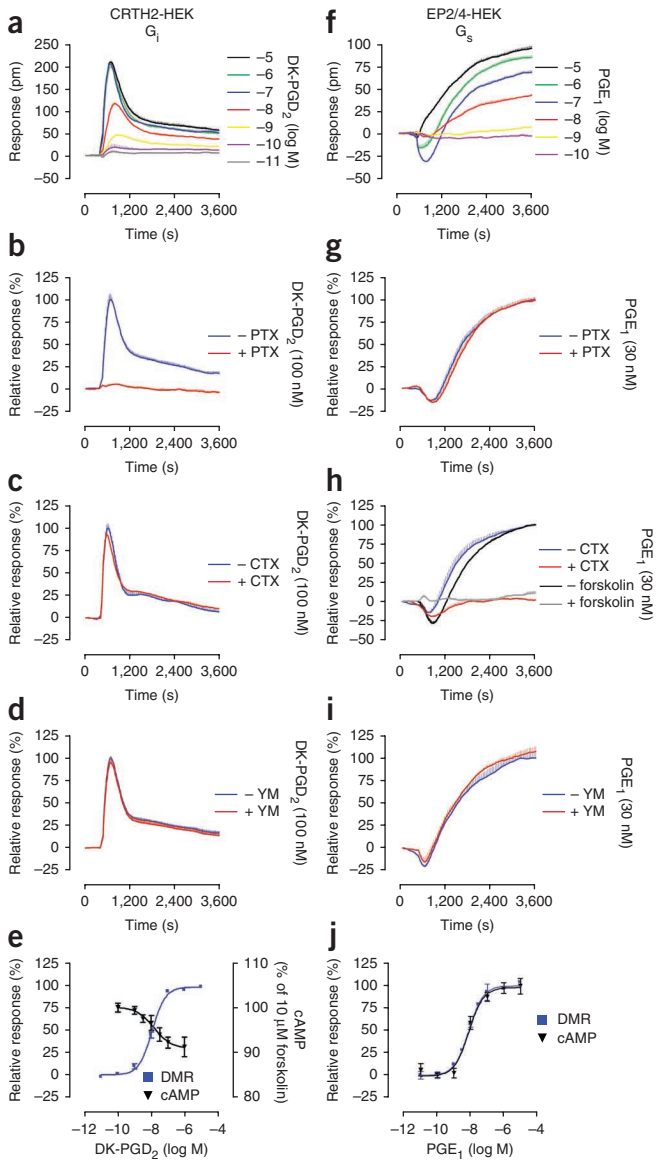

Figure 3 Dynamic mass redistribution enables measurement of differential receptor-mediated G protein activation in HEK293 cells. Shown are DMR and second-messenger assays performed with the following cell lines and receptors. (**a**–**e**) HEK293 cells stably expressing CRTH2. (**f**–**j**) HEK293 cells endogenously expressing EP2-EP4 receptors. In **a**,**f**, cells were challenged with the indicated concentrations of agonists and wavelength shift was monitored as a measure of receptor activation. Shown are representative data (mean + s.e.m.) of at least three independent experiments. In **b**,**g**, pretreatment of cells with 5 ng/ml PTX inhibits signaling of the G_i-sensitive CRTH2 receptor but not signaling of the G_s-sensitive EP2-EP4 receptors. In **c**,**h**, pretreatment of cells with 100 ng/ml CTX (or 10 µM forskolin) masks signaling of the G_s-sensitive EP2-EP4 receptors but does not affect G_i traces of CRTH2. In **d**,**i**, pretreatment of cells with 300 nM YM does not alter CRTH2 or EP2-EP4 traces. All data are normalized to the maximum response obtained in the absence of pharmacological inhibitors. In **e**,**j**, comparison of DMR assays with traditional cAMP second-messenger assays. In **e**, CRTH2-mediated decrease of intracellular cAMP is calculated as percent inhibition of adenylyl cyclase stimulated with 10 µM forskolin. Calculated log EC_{50} values are: (**e**) DMR: –7.96 ± 0.04, cAMP: –7.85 ± 0.34; (**j**) EP2-EP4–mediated responses in DMR and cAMP assays are normalized to the maximum responses obtained by 10 µM PGE_1 in each assay. Calculated log EC_{50} values are: DMR: –8.11 ± 0.07, cAMP: –8.11 ± 0.12. All data are means (±s.e.m.) of at least three independent experiments.

sufficient to completely erase the FFA1 response (**Fig. 4b**; compare black and red trace). Notably, however, G_i activity of FFA1 was barely detectable in traditional second-messenger cAMP inhibition assays (**Fig. 4d**), which is in good agreement with previous observations[35,36]. These findings highlight a strength of DMR technology: not only does DMR offer access to high content integrated cellular information, it also provides mechanistic insight if used in conjunction with inhibitors to deconvolute complex signaling pathways.

DMR can analyze GPCR function in human primary cells

Analyzing GPCR-mediated signal transduction in primary human cells—the cell type in which medicines are intended to mediate their therapeutic effect—is highly desirable for GPCR drug candidates. To test whether DMR is sufficiently sensitive to detect GPCR signaling in a native environment, we chose the cAMP-elevating agent PGE_1 as a stimulus, known to affect cell growth and cytokine production of human keratinocytes[39], and monitored DMR in both immortalized (HaCaT cells) and primary human keratinocytes obtained from six patients who underwent skin surgery. HaCaT and primary human keratinocytes responded with concentration-dependent optical traces reminiscent of those already observed in PGE_1-treated HEK293 cells (**Fig. 5a**,**b**; compare **Fig. 3f**). Indeed, PGE_1 traces in both HaCaT and primary human keratinocytes reflect activation of the two G_s-coupled EP2-EP4 receptors because the responses were sensitive to inhibition by a combination of EP2-EP4 antagonists (**Fig. 5c**,**d**), and were invisible following CTX- but not PTX- or YM-treatment (**Fig. 5e**,**f** and data not shown). Notably, although cAMP and DMR assays were both sufficiently sensitive to quantify PGE_1 activity in primary human cells, DMR was superior with respect to the quality of the signal window under conditions of low receptor expression (**Fig. 5g**,**h**).

DMR uncovers unknown signaling paradigms

It has been shown that persistent activation of the G_s signaling pathway can augment muscarinic M_3 receptor–mediated inositol phosphate production[40]. At first glance, the results reported here might appear to be in good accordance with this earlier report as we detected enhanced muscarinic M_3 receptor signaling in the presence of cAMP-elevating agents such as CTX (**Figs. 1g** and **6a**) and forskolin (**Fig. 6b**; red versus black trace). However, these enhanced M_3 signaling responses in DMR assays were sensitive to pretreatment of the cells with PTX, implying a G_i/G_o-mediated event (**Fig. 6a**,**b**; red versus blue trace). In contrast, M_3 DMR was completely insensitive to PTX pretreatment when intracellular cAMP was not elevated before application of the muscarinic agonist (**Fig. 6a**,**b**; gray versus black trace). These observations indicate that elevated intracellular cAMP—when present before the muscarinic agonist—serves as a stimulus to enable the M_3 receptor to engage an additional signaling pathway. Notably, detection of G_i activity under conditions of elevated cAMP can also be accomplished by immunocapture GTPγS binding assays (**Fig. 6c**) but not by traditional cAMP inhibition assays, in which receptor agonist and forskolin need to be co-applied simultaneously, not sequentially, to obtain measurable cAMP level changes as exemplified for the bona fide G_i-linked muscarinic M_2 receptor (**Supplementary Fig. 12**).

DISCUSSION

GPCRs constitute the single largest family of cell surface receptors, attracting great interest as therapeutic targets in all major disease

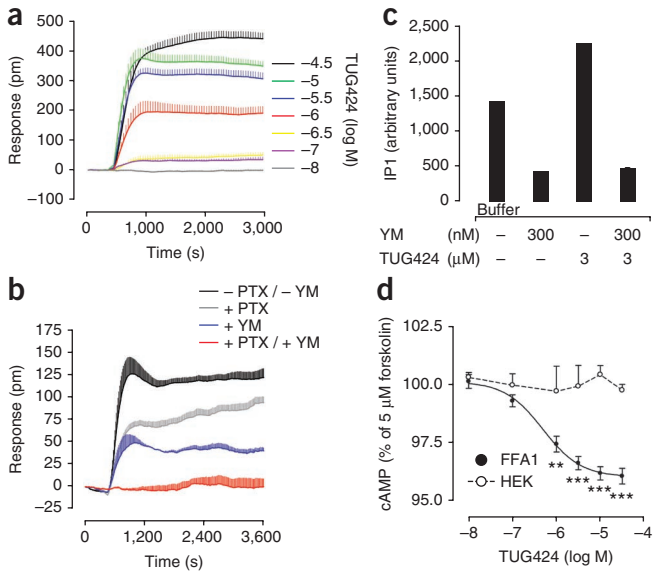

Figure 4 Parallel visualization of all signaling pathways unveils an additional signaling route of the free fatty acid receptor FFA1. (**a**) DMR recordings of FFA1-HEK cells treated with the indicated concentrations of the small-molecule agonist TUG424 (ref. 38). (**b**) The DMR signature obtained with 3 μM of the small-molecule FFA1 agonist TUG424 is partly sensitive to pretreatment of FFA1-HEK cells with PTX (5 ng/ml) or YM (300 nM) but completely abrogated in the presence of a combination of PTX and YM. (**c**) FFA1-mediated production of the second-messenger IP1 is completely blunted in the presence of 300 nM YM. FFA1-HEK cells were stimulated with 3 μM TUG424, and the resulting accumulation of inositol phosphates (IP1) was detected with an HTRF-IP1 assay kit as described in the Online Methods. (**d**) FFA1 activation of the G_i signaling pathway is statistically significant in cAMP inhibition assays. FFA1-HEK—or HEK293 cells for control—were stimulated with 5 μM forskolin, and inhibition of cAMP formation was quantified with an HTRF-cAMP assay kit as outlined in the Methods section. The cAMP level induced by stimulation with 5 μM forskolin (Fsk) was set to 100%. Shown are mean values and s.e.m. of three to six independent experiments. For statistical analysis, individual concentrations were compared by two-way ANOVA with Bonferroni's correction for multiple comparisons. $^{**}P < 0.01$, $^{***}P < 0.001$.

areas[1]. Accordingly, assay technologies enabling discovery of novel GPCR ligands are likely to substantially influence the drug discovery process. Recently, label-free technology platforms based on dynamic mass redistribution of intracellular proteins such as the Corning Epic Biosensor (for operating principle see **Fig. 1a**) or alteration of electric impedance have emerged for the study of GPCRs[5,22–25,41]. However, no in-depth analytical study to date has thoroughly 'validated' and/or compared the novel DMR technology with the more traditional biochemical and second-messenger assays that have been the mainstay of GPCR drug development.

Our results show that DMR technology can capture receptor activation of all four GPCR coupling classes (G_i/G_o, G_s, G_q and G_{12}/G_{13}), which at present is unachievable by most other technology platforms. DMR technology therefore represents a universal, pathway-unbiased yet pathway-sensitive approach toward investigation of G protein–mediated effects. The ability of the technology to detect signaling

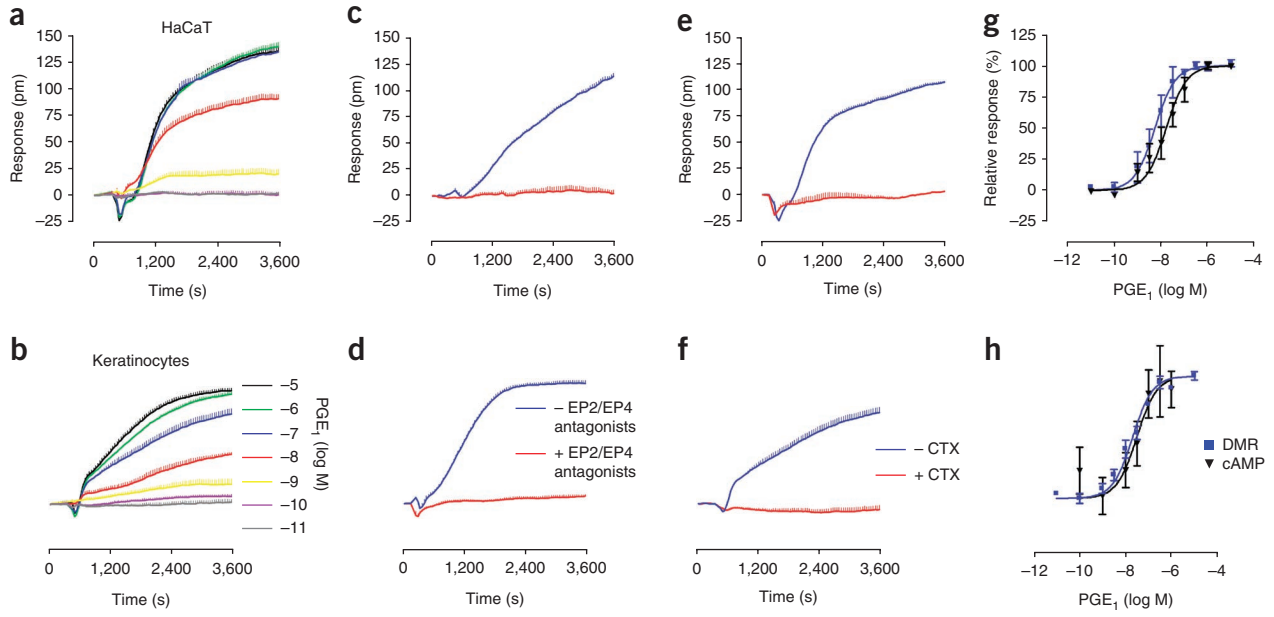

Figure 5 Dynamic mass redistribution enables analysis of GPCR functionality in immortalized and primary human keratinocytes. Top panels, immortalized human keratinocytes (HaCaTs); bottom panels, primary human keratinocytes. (**a**,**b**) The cell lines were challenged with the indicated concentrations of PGE_1, and wavelength shift over time was monitored as a measure of receptor activation. (**a**) Representative data (+ s.e.m.) of at least four independent experiments. (**b**) Representative data (+ s.e.m.) of cells from one human donor. Cells of five additional human donors yielded comparable optical traces (not shown). (**c**,**d**) PGE_1-mediated DMR is inhibited by pretreatment with a combination of the EP2-EP4 receptor antagonists AH6809 and L161,982, respectively. Optical traces of 30 nM PGE_1 (**c**) or 100 nM PGE_1 (**d**) in the absence and presence of a combination of 10 μM AH6809 and 3 μM L161,982. All data are representative data (+ s.e.m.) of at least four independent experiments. (**e**,**f**) DMR signatures of 100 nM PGE_1 are masked when cells are pretreated with 250 ng/ml cholera toxin (CTX). (**e**) Representative data (+ s.e.m.) of at least four independent experiments. (**f**) One representative dataset (+ s.e.m.) from one out of five human subjects. (**g**,**h**) Comparison of DMR assays with traditional endpoint cAMP second-messenger assays. Calculated log EC_{50} values are: (**g**) HaCaT: DMR: –8.27 ± 0.09, cAMP: –7.78 ± 0.09; (**h**) keratinocytes: DMR: –7.70 ± 0.06, cAMP: –7.60 ± 0.12. All data are means (±s.e.m.) of at least four independent experiments.

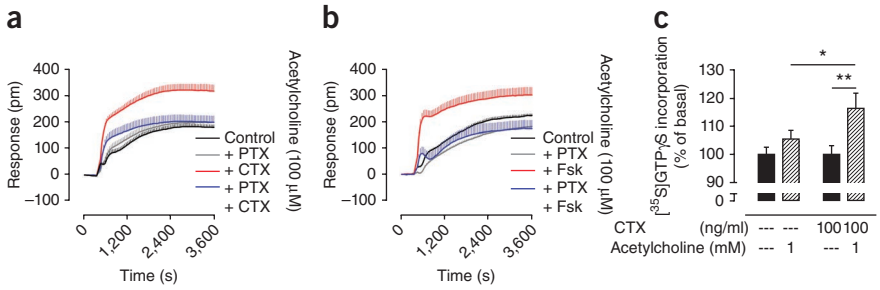

Figure 6 The muscarinic M_3 receptor adapts to adenylyl cyclase activation with a changed signaling repertoire. (**a**,**b**) Set of DMR experiments addressing (**a**) indirect and (**b**) direct activation of adenylyl cyclase by cholera toxin (CTX) and forskolin (Fsk), respectively. Acetylcholine (100 µM)-induced DMR traces were measured under control conditions and after pretreatment with pertussis toxin (100 ng/ml; PTX), CTX (100 ng/ml) or Fsk (10 µM) as indicated. Representative data (mean + s.e.m.) from at least three independent experiments. Note that PTX sensitivity emerges only after pretreatment with either CTX or forskolin. (**c**) GTPγS binding assay on membranes prepared from M_3-CHO cells. M_3-CHO cells were grown to confluence and were left untreated or were pretreated with CTX (20 h, 100 ng/ml) before membrane preparation. GTPγS incorporation was determined in the absence and presence of 1 mM acetylcholine followed by immunoenrichment of G_i proteins with an antiserum to the C-terminal region common to G_i proteins, as described in the Online Methods (mean + s.e.m., $n = 3$). *P* values <0.05 were considered statistically significant according to one-way analysis of variance (ANOVA) with Bonferroni's correction for multiple comparisons, as appropriate.

along the G_{12}/G_{13} pathway may be of great relevance to future 'GPCR deorphanization' strategies, particularly as receptors previously considered to be non-signaling might exclusively signal through G_{12}/G_{13}. Although lack of pathway bias is highly advantageous for deorphanization studies, the possibility must be considered that DMR traces, if opposing in direction and possessing identical kinetics, may yield zero signatures and therefore mask activity of biologically relevant molecules. Nevertheless, the use of pathway blockers should uncover such hidden pathway activation.

DMR technology and traditional second-messenger assays also diverge greatly in another aspect: DMR displays an overall cellular response, most likely encompassing a variety of cellular events downstream of the GPCR[5,22–24], which is in stark contrast to quantification of defined second messengers that only partially determine the overall response. This likely explains why agonist potencies determined with both methods may, but do not necessarily have to, converge. Indeed, this study revealed that the sensitivity of DMR is at least equal or even superior (**Fig. 1i**) to that of second-messenger recording for the detection of receptor-dependent, G protein–mediated signaling.

Complexity of optical traces obviously raises the possibility that an unimaginable wealth of intracellular players may be involved in defining the fine details of signature amplitude and duration. It will be exciting to unravel the individual components shaping complex optical response patterns, perhaps using libraries of signaling pathway inhibitors or genome-wide genetic screens with siRNA libraries. Our study does not solve the signature riddle completely, but provides a major mechanistic advance toward understanding the complex optical traces. Namely, heterotrimeric G proteins represent the postreceptor trigger responsible for orchestrating the complex response profiles for the various receptors and cellular backgrounds examined here, which was demonstrated using a combination of toxins and pharmacological pathway inhibitors.

The experimental power of these tools in label-free detection has been shown in this study for many different receptors and various cellular backgrounds, including primary human keratinocytes. Given the emerging successes in directing differentiation of embryonic or pluripotent stem cells to mature cells such as neurons or endothelial cells[42,43], label-free DMR detection raises the exciting possibility of expanding studies of drug action mechanisms and even drug screening processes to physiologically relevant cells. Native signaling has already been addressed in publications using label-free DMR detection[25]. All of these reports, however, have involved the analysis of immortalized cell lines[25], which are much less close to tissue biology than the primary human cells used here.

Our study also demonstrates how the collation of signaling routes within one dynamic, all-encompassing response, and its mechanistic deconvolution with appropriate pharmacological tools, can visualize unexpected signaling phenomena. Identification of an additional signaling pathway for the free fatty acid receptor FFA1 is one such example. In fact, the application of DMR technology to reveal ligand efficacy along the G_i pathway is particularly noteworthy because this aspect of FFA1 behavior is hardly detectable in the traditional cAMP inhibition assay (**Fig. 4d**). Identification of cAMP as an intracellular stimulus that confers signaling multiplicity onto the muscarinic M_3 receptor is another example. Although M_3-G_i interaction has been inferred indirectly many years ago on the basis of partial PTX sensitivity of M_3-mediated responses[44,45], a defined stimulus for this event has remained elusive so far. It is therefore important to stress that this particular mode of cellular cross-talk has been uncovered because DMR visualizes the summation of individual GPCR signaling routes during a single experiment, and because DMR, in contrast to traditional biochemical assays, does not require pharmacological manipulation of the second-messenger adenylyl cyclase–cAMP pathway to probe G protein (G_i) activity.

In summary, comparative analysis of traditional biochemical methods with the more recently developed DMR technology platform uncovers the experimental power of whole-cell label-free detection. Not only does DMR provide a temporally resolved readout for the summation of receptor-triggered signaling events in recombinant and primary living cells with unprecedented sensitivity and accuracy, but it is this cumulative readout of cellular activity that may disclose further levels of biological complexity in the regulation of signal transduction processes. We therefore anticipate that DMR, as a holistic readout of cell function, will advance systems biology and systems pharmacology and thereby promote the discovery of therapeutics with novel mechanisms.

METHODS

Methods and any associated references are available in the online version of the paper at http://www.nature.com/naturebiotechnology/.

Note: Supplementary information is available on the Nature Biotechnology website.

ACKNOWLEDGMENTS

We thank U. Rick, M. Vasmer-Ehses and T. Kögler for expert technical assistance and Corning Inc. for providing us with the Epic system. This work was supported by the DFG (Deutsche Forschungsgemeinschaft) grants KO 1582/3-1 to E.K., MO 821/2-1 to K.M. and WE 4428/1-1 to J.W. and by the Dr. Hilmer Foundation

(PhD fellowship to S.H.). A.K. is a member of the DFG-funded Research Training School GRK 677. N.J.S is an NHMRC/NHF of Australia Overseas Research Fellow. We thank M. De Amici and U. Holzgrabe (University of Milan and University of Würzburg) for kindly providing Hybrid 1 (ref. 47), T. Ulven (University of Southern Denmark) for TUG424 (ref. 38) and Astellas Pharma Inc. (Osaka, Japan) for providing us with YM-254890 (ref. 30).

AUTHOR CONTRIBUTIONS

R.S., N.J., J.S., A.K., N.M., S.H., A.M., S.B., M.M.-A. and N.J.S. designed and performed the experiments; E.K. and K.M. designed the research and wrote the manuscript; S.Z., J.W. and G.M. provided important biological samples or research tools; C.D., J.G., N.J.S., G.M. and R.S. provided important ideas and edited the manuscript.

COMPETING FINANCIAL INTERESTS

The authors declare competing financial interests: details accompany the full-text HTML version of the paper at http://www.nature.com/naturebiotechnology/.

Published online at http://www.nature.com/naturebiotechnology/.
Reprints and permissions information is available online at http://npg.nature.com/reprintsandpermissions/.

1. Overington, J.P., Al-Lazikani, B. & Hopkins, A.L. How many drug targets are there? *Nat. Rev. Drug Discov.* **5**, 993–996 (2006).
2. Baker, J.G. & Hill, S.J. Multiple GPCR conformations and signalling pathways: implications for antagonist affinity estimates. *Trends Pharmacol. Sci.* **28**, 374–381 (2007).
3. Bosier, B. & Hermans, E. Versatility of GPCR recognition by drugs: from biological implications to therapeutic relevance. *Trends Pharmacol. Sci.* **28**, 438–446 (2007).
4. Galandrin, S., Oligny-Longpre, G. & Bouvier, M. The evasive nature of drug efficacy: implications for drug discovery. *Trends Pharmacol. Sci.* **28**, 423–430 (2007).
5. Kenakin, T.P. Cellular assays as portals to seven-transmembrane receptor-based drug discovery. *Nat. Rev. Drug Discov.* **8**, 617–626 (2009).
6. Urban, J.D. *et al.* Functional selectivity and classical concepts of quantitative pharmacology. *J. Pharmacol. Exp. Ther.* **320**, 1–13 (2007).
7. Kenakin, T. Agonist-receptor efficacy. II. Agonist trafficking of receptor signals. *Trends Pharmacol. Sci.* **16**, 232–238 (1995).
8. Ryberg, E. *et al.* The orphan receptor GPR55 is a novel cannabinoid receptor. *Br. J. Pharmacol.* **152**, 1092–1101 (2007).
9. Eglen, R.M. Functional G protein-coupled receptor assays for primary and secondary screening. *Comb. Chem. High Throughput Screen.* **8**, 311–318 (2005).
10. Williams, C. cAMP detection methods in HTS: selecting the best from the rest. *Nat. Rev. Drug Discov.* **3**, 125–135 (2004).
11. Willoughby, D. & Cooper, D.M. Live-cell imaging of cAMP dynamics. *Nat. Methods* **5**, 29–36 (2008).
12. Barnea, G. *et al.* The genetic design of signaling cascades to record receptor activation. *Proc. Natl. Acad. Sci. USA* **105**, 64–69 (2008).
13. Hamdan, F.F., Audet, M., Garneau, P., Pelletier, J. & Bouvier, M. High-throughput screening of G protein-coupled receptor antagonists using a bioluminescence resonance energy transfer 1-based β-arrestin2 recruitment assay. *J. Biomol. Screen.* **10**, 463–475 (2005).
14. Lefkowitz, R.J. & Whalen, E.J. β-arrestins: traffic cops of cell signaling. *Curr. Opin. Cell Biol.* **16**, 162–168 (2004).
15. Olson, K.R. & Eglen, R.M. β-galactosidase complementation: a cell-based luminescent assay platform for drug discovery. *Assay Drug Dev. Technol.* **5**, 137–144 (2007).
16. Verkaar, F. *et al.* G protein-independent cell-based assays for drug discovery on seven-transmembrane receptors. *Biotechnol. Annu. Rev.* **14**, 253–274 (2008).
17. Azzi, M. *et al.* β-arrestin-mediated activation of MAPK by inverse agonists reveals distinct active conformations for G protein-coupled receptors. *Proc. Natl. Acad. Sci. USA* **100**, 11406–11411 (2003).
18. Galandrin, S. & Bouvier, M. Distinct signaling profiles of β1 and β2 adrenergic receptor ligands toward adenylyl cyclase and mitogen-activated protein kinase reveals the pluridimensionality of efficacy. *Mol. Pharmacol.* **70**, 1575–1584 (2006).
19. Hansen, J.L., Theilade, J., Haunso, S. & Sheikh, S.P. Oligomerization of wild type and nonfunctional mutant angiotensin II type I receptors inhibits $G\alpha_q$ protein signaling but not ERK activation. *J. Biol. Chem.* **279**, 24108–24115 (2004).
20. Hoffmann, C., Ziegler, N., Reiner, S., Krasel, C. & Lohse, M.J. Agonist-selective, receptor-specific interaction of human P2Y receptors with β-arrestin-1 and -2. *J. Biol. Chem.* **283**, 30933–30941 (2008).
21. Violin, J.D. & Lefkowitz, R.J. β-arrestin-biased ligands at seven-transmembrane receptors. *Trends Pharmacol. Sci.* **28**, 416–422 (2007).
22. Fang, Y., Ferrie, A.M., Fontaine, N.H., Mauro, J. & Balakrishnan, J. Resonant waveguide grating biosensor for living cell sensing. *Biophys. J.* **91**, 1925–1940 (2006).
23. Fang, Y., Li, G. & Ferrie, A.M. Non-invasive optical biosensor for assaying endogenous G protein-coupled receptors in adherent cells. *J. Pharmacol. Toxicol. Methods* **55**, 314–322 (2007).
24. Fang, Y. & Ferrie, A.M. Optical biosensor differentiates signaling of endogenous PAR1 and PAR2 in A431 cells. *BMC Cell Biol.* **8**, 24 (2007).
25. Rocheville, M. & Jerman, J.C. 7TM pharmacology measured by label-free: a holistic approach to cell signalling. *Curr. Opin. Pharmacol.* **9**, 643–649 (2009).
26. Dodgson, K., Gedge, L., Murray, D.C. & Coldwell, M. A 100K well screen for a muscarinic receptor using the Epic label-free system—a reflection on the benefits of the label-free approach to screening seven-transmembrane receptors. *J. Recept. Signal Transduct. Res.* **29**, 163–172 (2009).
27. Lee, P.H. *et al.* Evaluation of dynamic mass redistribution technology for pharmacological studies of recombinant and endogenously expressed G protein-coupled receptors. *Assay Drug Dev. Technol.* **6**, 83–94 (2008).
28. McGuinness, R.P. *et al.* Enhanced selectivity screening of GPCR ligands using a label-free cell based assay technology. *Comb. Chem. High Throughput Screen.* **12**, 812–823 (2009).
29. Peters, M.F., Vaillancourt, F., Heroux, M., Valiquette, M. & Scott, C.W. Comparing label-free biosensors for pharmacological screening with cell-based functional assays. *Assay Drug Dev. Technol.* **8**, 219–227 (2010).
30. Takasaki, J. *et al.* A novel $G\alpha_q$/11-selective inhibitor. *J. Biol. Chem.* **279**, 47438–47445 (2004).
31. Riobo, N.A. & Manning, D.R. Receptors coupled to heterotrimeric G proteins of the G12 family. *Trends Pharmacol. Sci.* **26**, 146–154 (2005).
32. Henstridge, C.M. *et al.* The GPR55 ligand l-α-lysophosphatidylinositol promotes RhoA-dependent Ca^{2+} signaling and NFAT activation. *FASEB J.* **23**, 183–193 (2009).
33. Ross, R.A. The enigmatic pharmacology of GPR55. *Trends Pharmacol. Sci.* **30**, 156–163 (2009).
34. Henstridge, C.M. *et al.* GPR55 ligands promote receptor coupling to multiple signalling pathways. *Br. J. Pharmacol.* **160**, 604–614 (2010).
35. Briscoe, C.P. *et al.* The orphan G protein-coupled receptor GPR40 is activated by medium and long chain fatty acids. *J. Biol. Chem.* **278**, 11303–11311 (2003).
36. Itoh, Y. *et al.* Free fatty acids regulate insulin secretion from pancreatic beta cells through GPR40. *Nature* **422**, 173–176 (2003).
37. Stoddart, L.A., Brown, A.J. & Milligan, G. Uncovering the pharmacology of the G protein-coupled receptor GPR40: high apparent constitutive activity in guanosine 5′-*O*-(3-[^{35}S]thio)triphosphate binding studies reflects binding of an endogenous agonist. *Mol. Pharmacol.* **71**, 994–1005 (2007).
38. Christiansen, E. *et al.* Discovery of potent and selective agonists for the free fatty acid receptor 1 (FFA(1)/GPR40), a potential target for the treatment of type II diabetes. *J. Med. Chem.* **51**, 7061–7064 (2008).
39. Zhang, J.Z., Maruyama, K., Iwatsuki, K., Ono, I. & Kaneko, F. Effects of prostaglandin E1 on human keratinocytes and dermal fibroblasts: a possible mechanism for the healing of skin ulcers. *Exp. Dermatol.* **3**, 164–170 (1994).
40. McGraw, D.W., Almoosa, K.F., Paul, R.J., Kobilka, B.K. & Liggett, S.B. Antithetic regulation by β-adrenergic receptors of G_q receptor sinaling via phospholipase C underlies the airway beta-agonist paradox. *J. Clin. Invest.* **112**, 619–626 (2003).
41. McGuinness, R. Impedance-based cellular assay technologies: recent advances, future promise. *Curr. Opin. Pharmacol.* **7**, 535–540 (2007).
42. Gaspard, N. *et al.* Generation of cortical neurons from mouse embryonic stem cells. *Nat. Protoc.* **4**, 1454–1463 (2009).
43. James, D. *et al.* Expansion and maintenance of human embryonic stem cell-derived endothelial cells by TGFβ inhibition is Id1 dependent. *Nat. Biotechnol.* **28**, 161–166 (2010).
44. Burford, N.T., Tobin, A.B. & Nahorski, S.R. Differential coupling of m1, m2 and m3 muscarinic receptor subtypes to inositol 1,4,5-trisphosphate and adenosine 3′,5′-cyclic monophosphate accumulation in Chinese hamster ovary cells. *J. Pharmacol. Exp. Ther.* **274**, 134–142 (1995).
45. Schmidt, M., Nehls, C., Rumenapp, U. & Jakobs, K.H. m3 Muscarinic receptor-induced and Gi-mediated heterologous potentiation of phospholipase C stimulation: role of phosphoinositide synthesis. *Mol. Pharmacol.* **50**, 1038–1046 (1996).

ONLINE METHODS

Materials and reagents. Tissue culture media reagents were from Invitrogen or Sigma-Aldrich, prostaglandin E_1 (PGE_1), 13,14-dihydro-15-keto-prostaglandin D_2 (DK-PGD_2) and AH6809 from Cayman, L161,982 from Tocris, forskolin (Fsk) from Applichem, [^{35}S]GTPγS from Perkin Elmer and Hank's balanced salt solution (HBSS) from Invitrogen. All other chemicals were obtained from Sigma-Aldrich unless explicitly indicated.

Cell culture and cell lines stably expressing individual GPCRs. The following receptors (human sequences) and cell lines were used: Flp-In-Chinese hamster ovary cells (Flp-In-CHO) stably expressing the M_2 or the M_3 receptor referred herein as M_2-CHO and M_3-CHO, CHO cells stably expressing the GPR55 or the β_2 receptor (GPR55-CHO and β_2-CHO) and untransfected CHO cells. CHO cells were cultured in Ham's nutrient mixture F-12 (HAM-F12) supplemented with 10% (v/v) FCS (FCS), 100 U/ml penicillin, 100 µg/ml streptomycin. The medium was complemented with 2 mM L-glutamine for M_2-CHO and M_3-CHO, 1 mM L-glutamine and 200 µg/ml G418 for β_2-CHO and 400 µg/ml G418 for GPR55-CHO.

HEK293 cells and HEK293 cells stably expressing CRTH2 (CRTH2-HEK cells), HEK293-Flp-In T-REx cells stably transfected with FFA1 (FFA1-HEK) and AD-HEK293 stably transfected with 3xHA-GPR55 (GPR55-HEK, kindly provided by Andrew Irving, University of Dundee, UK) were cultured in Dulbecco's modified Eagle's medium (DMEM) supplemented with 10% (v/v) FCS, 100 U/ml penicillin and 100 µg/ml streptomycin. For CRTH2-HEK and GPR55-HEK the medium was supplemented with 500 µg/ml G418, and for FFA1-HEK with 100 µg/ml hygromycin B and 15 µg/ml blasticidin (both from InvivoGen). For receptor expression FFA1-HEK cells were treated with 1 µg/ml doxycycline for 16 h.

Immortalized keratinocytes (human adult low calcium temperature, or HaCaT, cells) were grown in RPMI-1640 supplemented with 10% (v/v) FCS, 100 U/ml penicillin and 100 µg/ml streptomycin.

Primary human keratinocytes were obtained from skin samples of healthy patients and were cultured in KGM2 (Promocell) supplemented with 100 U/ml penicillin and 100 µg/ml streptomycin. All patients had provided written informed consent before excision. The study was approved by the ethics committee of the University of Bonn (concession-no. 090/04).

All cells were cultivated with 5% CO_2 at 37 °C.

Transient transfections of GPR55-HEK cells. To effectively deliver cDNA coding for dominant-negative G13 (G13Q226L,D294N) into GPR55-HEK cells an electroporation method was used as described previously[46]. DMR measurements were performed 48 h after transfection.

Dynamic mass redistribution (DMR) assays (Corning Epic Biosensor measurements). A beta version of the Corning Epic System was used consisting of a temperature-control unit, an optical detection unit, and an on-board robotic liquid handling device. Functional principle: a confluent cell layer adheres to the bottom of a well equipped with an optical biosensor. Ingoing broadband light is directed to travel along the bottom. The electromagnetic field extends into the cell layer for a depth of about 150 nm and loses energy depending on the optical density of the adjacent cell area, and the outgoing wavelength is measured. GPCR-mediated signaling affects optical density and thereby shifts the outgoing wavelength (measured in picometers) relative to pre-stimulus condition and is recorded over time. The magnitude of this wavelength shift is proportional to the amount of relocated intracellular matter: an increase in mass contributes positively and a decrease negatively to the overall response[22,23].

Cells were seeded onto 384-well Epic sensor microplates and cultured for 20–24 h to obtain confluent monolayers. GPR55 cells were treated as described previously[34].

Before the assay, cells were washed with assay buffer (HBSS with 20 mM HEPES) and transferred to the Epic reader for 2 h at 28 °C. DMR was monitored before and after addition of compound solutions. The incubation time for pretreatment with PTX or CTX was 16–20 h, for YM-254890 2.5 h, for aluminum fluoride 1.5 h and for forskolin 1–2.5 h.

[^{35}S]GTPγS assay. Membranes were prepared from M_2-CHO cells and [^{35}S]GTPγS incorporation measured as described previously[47,48]. For muscarinic M_3 receptors [^{35}S]GTPγS binding assays included an immunocapture step with an antiserum to the C terminus of G_i and were performed according to a previously published procedure[49].

Second-messenger accumulation assays (over expressed receptors). cAMP and IP1 accumulation were quantified with the HTRF-cAMP dynamic kit or the HTRF-IP1 kit, respectively (both from Cisbio) as per manufacturer's instructions and as described previously[50] on a Mithras LB 940 reader (Berthold Technologies).

cAMP accumulation assay (endogenously expressed receptors). cAMP accumulation was quantified with the competitive immunoassay HitHunter cAMP-HS+-kit (DiscoveRx Corp.) as per manufacturer's instructions using the Mithras LB 940 reader.

Calculations and data analysis. Quantification of DMR signals for concentration effect curves was performed either by calculation of the area under the curve (AUC) between 0 and 3,600 s (**Figs. 1i**,**j**, **2b**,**f**, **3j** and **5g**,**h**) or by the maximum value between 300 and 1,200 s (**Figs. 1h** and **3e**) for those traces that displayed fast kinetics and clear peak maxima. All optical DMR recordings were buffer and solvent corrected. For data normalization, indicated as relative response (%), top levels of concentration effect curves were set 100% and bottom levels 0%. Data calculation and EC_{50} value determination by nonlinear regression was performed using GraphPad Prism 4.02 (GraphPad Software).

Statistical analysis. Where appropriate, differences in means were examined by one- or two-way analysis of variance (ANOVA) with Bonferroni's multiple comparison post-hoc test using GraphPad Prism 5.01 (GraphPad Software). A P value <0.05 was considered statistically significant.

46. Pantaloni, C. *et al.* Alternative splicing in the N-terminal extracellular domain of the pituitary adenylate cyclase-activating polypeptide (PACAP) receptor modulates receptor selectivity and relative potencies of PACAP-27 and PACAP-38 in phospholipase C activation. *J. Biol. Chem.* **271**, 22146–22151 (1996).
47. Antony, J. *et al.* Dualsteric GPCR targeting: a novel route to binding and signaling pathway selectivity. *FASEB J.* **23**, 442–450 (2009).
48. Jäger, D. *et al.* Allosteric small molecules unveil a role of an extracellular E2/transmembrane helix 7 junction for G protein-coupled receptor activation. *J. Biol. Chem.* **282**, 34968–34976 (2007).
49. Smith, N.J., Stoddart, L.A., Devine, N.M., Jenkins, L. & Milligan, G. The action and mode of Binding of thiazolidinedione ligands at free fatty acid receptor 1. *J. Biol. Chem.* **284**, 17527–17539 (2009).
50. Schröder, R. *et al.* The C-terminal tail of CRTH2 is a key molecular determinant that constrains $G\alpha_i$ and downstream signaling cascade activation. *J. Biol. Chem.* **284**, 1324–1336 (2009).

doi:10.1038/nbt.1671